Available online at www.sciencedirect.com
ScienceDirect
Ceramics International 35 (2009) 3013–3019
CERAMICS INTERNATIONAL
www.elsevier.com/locate/ceramint

Synthesis and properties of lithium disilicate glass-ceramics in the system SiO_2–Al_2O_3–K_2O–Li_2O

D.U. Tulyaganov [a,b], S. Agathopoulos [c], I. Kansal [a], P. Valério [d], M.J. Ribeiro [e], J.M.F. Ferreira [a,*]

[a] Department of Ceramics and Glass Engineering, University of Aveiro, CICECO, 3810-193 Aveiro, Portugal
[b] State Committee of Geology and Mineral Resources, Centre of remote sensing and GIS technologies, 11-A, Shevchenko, str., 100060, Tashkent, Uzbekistan
[c] Department of Materials Science and Engineering, University of Ioannina, GR-451 10 Ioannina, Greece
[d] Department of Biophysics and Physiology, Federal University of Minas Gerais, ICB-UFMG, 31270-901 Belo Horizonte, Brazil
[e] UIDM, ESTG, Polytechnic Institute of Viana do Castelo, 4900 Viana do Castelo, Portugal

Received 2 March 2009; received in revised form 13 March 2009; accepted 2 April 2009
Available online 3 May 2009

Abstract

The purpose of this study was the synthesis of lithium disilicate glass-ceramics in the system SiO_2–Al_2O_3–K_2O–Li_2O. A total of 8 compositions from three series were prepared. The starting glass compositions 1 and 2 were selected in the leucite–lithium disilicate system with leucite/lithium disilicate weight ratio of 50/50 and 25/75, respectively. Then, production of lithium disilicate glass-ceramics was attempted via solid-state reaction between Li_2SiO_3 (which was the main crystalline phase in compositions 1 and 2) and SiO_2. In the second series of compositions, silica was added to fine glass powders of the compositions 1 and 2 (in weight ratio of 20/100 and 30/100) resulting in the modified compositions 1–20, 1–30, 2–20, and 2–30. In the third series of compositions, excess of silica, in the amount of 30 wt.% and 20 wt.% with respect to the parent compositions 1 and 2, was introduced directly into the glass batch. Specimens, sintered at 800 °C, 850 °C and 900 °C, were tested for density (Archimedes' method), Vickers hardness (H_V), flexural strength (3-point bending tests), and chemical durability. Field emission scanning electron microscopy and X-ray diffraction were employed for crystalline phase analysis of the glass-ceramics. Lithium disilicate precipitated as dominant crystalline phase in the crystallized modified compositions containing colloidal silica as well as in the glass-ceramics 3 and 4 after sintering at 850 °C and 900 °C. Self-glazed effect was observed in the glass-ceramics with compositions 3 and 4, whose 3-point bending strength and microhardness values were 165.3 (25.6) MPa and 201.4 (14.0) MPa, 5.27 (0.48) GPa and 5.34 (0.40) GPa, respectively.

Keywords: A. Sintering; D. Glass; D. Glass ceramics; D. Silicate; Lithium disilicate

1. Introduction

The evolution of ceramics technology has vastly contributed to the improvement of the quality of dental materials. Application of efficient processing and manufacturing can result in dental restorative materials with low production cost, high aesthetics, and long-term good mechanical and chemical performance after implantation [1,2]. The development of leucite (L, $KAlSi_2O_6$) and lithium disilicate (LD, $Li_2Si_2O_5$) glass-ceramics (GCs) has been a milestone at that respect [1–3].

The GCs of L are produced by controlled crystallization of glasses from the SiO_2–Al_2O_3–K_2O system via special heat treatments [4], or addition of synthetic L to powdered glass [5], or blending of a high expansion L-containing frit with a low expansion glass frit [6]. Dental prostheses manufacturing of L-containing GCs has involved sintering [7], heat pressing [8], and computer aided design and machining (CAD/CAM) [9], such as the IPS Empress® L-containing GC, produced via hot pressing, which fulfils the high aesthetic standards of dental restorations (inlays, onlays, crowns, veneers) [10].

The SiO_2–Li_2O system has attracted great interest due to the fundamental research of Stookey on the stoichiometric composition of layered phyllosilicate $Li_2Si_2O_5$ [1]. Since then, many comprehensive studies [11–16] led the development of

* Corresponding author. Tel.: +351 234 370242; fax: +351 234 425300.
E-mail address: jmf@ua.pt (J.M.F. Ferreira).

0272-8842/$36.00
doi:10.1016/j.ceramint.2009.04.002

LD GCs from a variety of systems. Chemical durability, which is of major importance for dental materials, was improved via adding Al_2O_3 and K_2O to stoichiometric LD-glass [17,18], or by developing GCs with non-stoichiometric (with respect to LD) compositions [1]. Introduction of SiO_2-excess to stoichiometric LD-glass along with additives, such as ZrO_2, Al_2O_3, ZnO, CaO, K_2O, and P_2O_5, has been suggested by Echeverria and Beall [19–21] for developing LD GCs for various applications. Later, P_2O_5 was found to play a crucial role in LD transformation and crystallization [22,23]. P_2O_5 (as nucleating agent) at the amount of 1.5–2.5 mol% resulted in GCs with fine-grained interlocking microstructures, conferring the final products with high mechanical strength.

A powder processing of LD GCs in a multi-component system with a wide compositional range of (in wt.%) 57–80 SiO_2, 11–19 Li_2O, 0–13 K_2O, 0–5 Al_2O_3, 0–8 ZnO, 0.1–6 La_2O_3, and 0.1–11 P_2O_5, was thoroughly investigated by Ivoclar-Vivadent company to produce the material IPS Empress®2 [24]. IPS Empress®2 is produced similarly to IPS Empress® GC via hot pressing. Höland et al. [10], Frank et al. [25], and Schweiger et al. [26] have reported its properties. That LD (65 vol.%) GC has a very dense microstructure, which comprises crystals of 1–2 μm in size embedded in a glassy matrix. High strength, translucent IPS Empress®2 GC is suitable for use as a metal-free framework material for dental crowns and three-unit bridges for anterior teeth [10].

The reaction mechanism in the GC powders, used for the synthesis of LD GCs, is complex [1,27]. In Al_2O_3-containing GCs, the predominant crystallization of $Li_2Si_2O_5$ occurs via the precursor lithium metasilicate (LS, Li_2SiO_3). In the Al_2O_3-free glass composition of (in mol.%) 63.2 SiO_2, 29.1 Li_2O, 2.9 K_2O, 3.3 ZnO, and 1.5 P_2O_5, both LS and LD form as primary crystalline phases at ca. 600 °C [28]. The growth of LD increases at 680 °C, due to the solid-state reaction of the chemical equation (1):

$$Li_2SiO_3 + SiO_2 \rightarrow Li_2Si_2O_5 \quad (1)$$

The machineability features of LS has motivated the production of GCs in the composition range of (in wt.%) 64–73 SiO_2, 13–17 Li_2O, 0.5–5 Al_2O_3, 2–5 K_2O, and 2–5 P_2O_5, via CAD/CAM, where machining is applied at the early stage of production, when crystallization of LS is predominant. Further heat treatment causes crystallization of LD, according to Eq. (1), resulting in high-strength LD GCs [29].

Accordingly, the acquired experience and scientific knowledge demonstrate high potential of compositions based on L and LD in dentistry. Furthermore, their manufacturing process is of crucial importance for producing dental GC materials with attractive properties and hence potential in clinical applications.

The present work presents a novel approach for the synthesis of LD GCs via powder processing, sintering and crystallization of glasses in the quaternary SiO_2–Al_2O_3–K_2O–Li_2O system with no addition of nucleating agents. The feasibility of the solid-state reaction between LS and silica to LD, according to Eq. (1), has been examined. The experimental results and their discussion are specially addressed to the crystallization behaviour of the glasses, the properties, and the microstructure of the sintered GCs, which confer to the new compositions potential relevance for producing dental materials.

Table 1
Batch compositions of glasses in wt.%.

Compositions	Li_2O	K_2O	Al_2O_3	SiO_2
1	9.95	10.79	11.68	67.58
1–20	8.29	8.99	9.73	72.98
1–30	7.65	8.30	8.98	75.06
2	14.93	5.39	5.84	73.84
2–20	12.44	4.49	4.87	78.20
2–30	11.48	4.15	4.49	79.88

The compositions 3 and 4 are the same with the compositions 1–30 and 2–20, respectively.

2. Materials and experimental procedure

Three series of compositions were investigated (Table 1). Two model glass compositions were initially selected in the L–LD system, with L/LD weight ratios of 50/50 and 25/75, designated as compositions 1 and 2, respectively. As it will be shown in Section 3, Li_2SiO_3 was the main crystalline phase in the GCs 1 and 2. Thus, in the second series of compositions, we considered the need of the presence of an excess of silica, testing, therefore, the feasibility of producing LD GCs according to Eq. (1). Suspension of colloidal silica was admixed with fine glass powders of the glasses 1 and 2 in a SiO_2/glass weight ratio of 20/100 and 30/100. The resultant compositions are designated as 1–20, 1–30, 2–20, and 2–30. In the third series of samples, we directly introduced the excess of silica in the initial glass batch and we produced two compositions, designated as 3 and 4, which had the same chemical compositions with 1–30 and 2–20, respectively.

Commercial powders of SiO_2 (Sibelco Portuguesa, Lda, Rio Maior, Portugal) and Al_2O_3 (Alcoa Chemicals, Arlington, TX, USA), and reactive grade K_2CO_3 and Li_2CO_3 (Sigma–Aldrich Química, S.A. Sintra, Portugal) were used. Reactive grade 50 wt.% suspension of colloidal silica in water (TM-50 Dupoint product, Aldrich Chemical Company, Inc.) was also used.

Regarding the glasses 1–4, homogeneous mixtures of batches (∼100 g), obtained by ball milling, were heated at 800 °C for 1 h in air for decarbonization and then melted in alumina crucibles at 1470–1550 °C (depending on the composition) for 1–2 h, in air. Glasses in bulk form were produced by pouring the melts on preheated bronze molds following by annealing at 500 °C for 1 h. Samples of glass-powder compacts were produced from glass frit, which was obtained by quenching of the glass melts in cold water. The frit was dried and then milled in a high-speed agate mill. The fine glass powders, having mean particle size of 4–5 μm (determined by light scattering technique, Coulter LS 230, UK, Fraunhofer optical model), were granulated (by stirring in a mortar) in a 5 vol.% polyvinyl alcohol solution (PVA, Merck; the solution of PVA was made by dissolution in warm water) in a proportion of 97.5 wt.% of glass powder and 2.5 wt.% of PVA solution. Rectangular bars with dimensions of 4 mm × 5 mm × 50 mm were prepared by uniaxial pressing (80 MPa). The bars

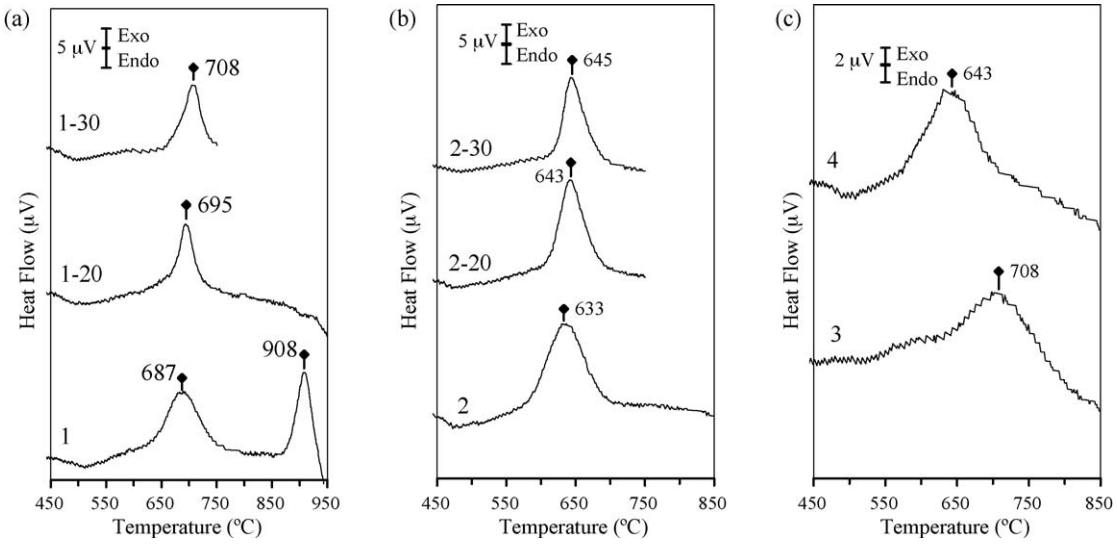

Fig. 1. Differential thermal analysis (DTA) of the investigated glasses.

were sintered in air for 1 h at 800 °C, 850 °C, and 900 °C. A slow heating rate of 2 K/min aimed to prevent deformation of samples.

To produce the compositions 1–20, 1–30, 2–20, and 2–30, appropriate amount of suspension of colloidal silica was admixed and homogenized with fine glass-powders 1 and 2 (obtained from the frits of the glasses 1 and 2). Pellets of 20 mm in diameter and 5 mm in height were sintered at 800 °C, 850 °C, and 900 °C, for 1 h in air.

The coefficients of thermal expansion (CTE) of the GCs were determined by dilatometry using prismatic samples with cross-section of 3 mm × 4 mm (Bahr Thermo Analyse DIL 801 L, Germany; heating rate 5 K/min). Differential thermal analysis of fine powders was carried out in air (DTA-TG, Labsys Setaram, France; heating rate 5 K/min). The crystalline phases were determined by X-ray diffraction (XRD) analysis (Rigaku Geigerflex D/Mac, C Series, Cu K_α radiation, Japan). Copper K_α radiation ($\lambda = 1.5406$ Å), produced at 30 kV and 25 mA, scanned the range of diffraction angles (2θ) between 10° and 60° with a 2θ-step of 0.02°/s. The phases were identified by comparing the obtained diffractograms with patterns of standards complied by the International Centre for Diffraction Data (ICDD). Microstructure observations were done at polished (mirror finishing) and then etched (by immersion in 2 vol.% HF solution for 5 min) surfaces of samples by field emission scanning electron microscopy (FE-SEM, Hitachi S-4100, Japan; 25 kV acceleration voltage, beam current 10 μA) under secondary electron mode. Archimedes' method (i.e. immersion in diethyl phthalate) was employed to measure the apparent density of the samples. The evaluation of mechanical properties comprised measurements of Vickers microhardness (Shimadzu microhardness tester type M, Japan, load of 200 g), and 3-point bending strength of rectified parallelepiped bars (3 mm × 4 mm × 50 mm) of sintered GCs (Shimadzu Autograph AG 25 TA, 0.5 mm/min displacement). The linear shrinkage during sintering was calculated from the difference of the dimensions between the green and the sintered bars. Chemical durability was determined by immersing samples, with diameter of 16.5 mm and thickness of 1.6 mm, in 4 vol.% acetic acid solution and boiling at 80 °C for 16 h and 32 h.

3. Results

Melting at 1470 °C and 1500 °C for 1 h was adequate to obtain transparent and colourless molten glasses 1 and 2, respectively. Nevertheless, visible bubbles were evident in glass 2, which almost disappeared after re-melting of glass frit at 1550 °C for 1 h. Two pronounced crystallization peaks at 687 °C and 908 °C were observed in the DTA plot of glass 1 and only one peak for glass 2 at 633 °C (Fig. 1).

Sintering of the glass-powder compacts at 800 °C resulted in highly dense samples of white colour. Further increase of temperature up to 850 °C or 900 °C negligibly influenced the shape and the colour of the samples. The values of shrinkage, density, and bending strength of glass-powder compacts of the compositions 1 and 2, sintered at 800 °C, 850 °C and 900 °C for 1 h, are summarized in Table 2.

The X-ray diffractograms of GC 1 after sintering at 800 °C, 850 °C, and 900 °C, for 1 h are shown in Fig. 2a. Lithium

Table 2
Property mean values and (standard deviation – SD) of glass-ceramics 1 and 2 sintered at different temperatures.

Property	T (°C)	1	2
Density (g/cm^3)	800	2.38 (0.01)	2.35 (0.01)
	850	2.37 (0.01)	2.350 (0.01)
	900	2.38 (0.01)	2.300 (0.01)
Shrinkage (%)	800	15.6 (0.1)	14.5 (0.2)
	850	15.7 (0.1)	14.9 (0.1)
	900	15.6 (0.3)	14.6 (0.1)
3-Point bending strength (MPa)	800	105.1 (10.9)	105.2 (16.5)
	850	129.6 (12.6)	134.0 (13.8)
	900	116.6 (10.8)	154.6 (9.7)

The results were obtained from 10 different independent samples and are the case of bending strength 10.

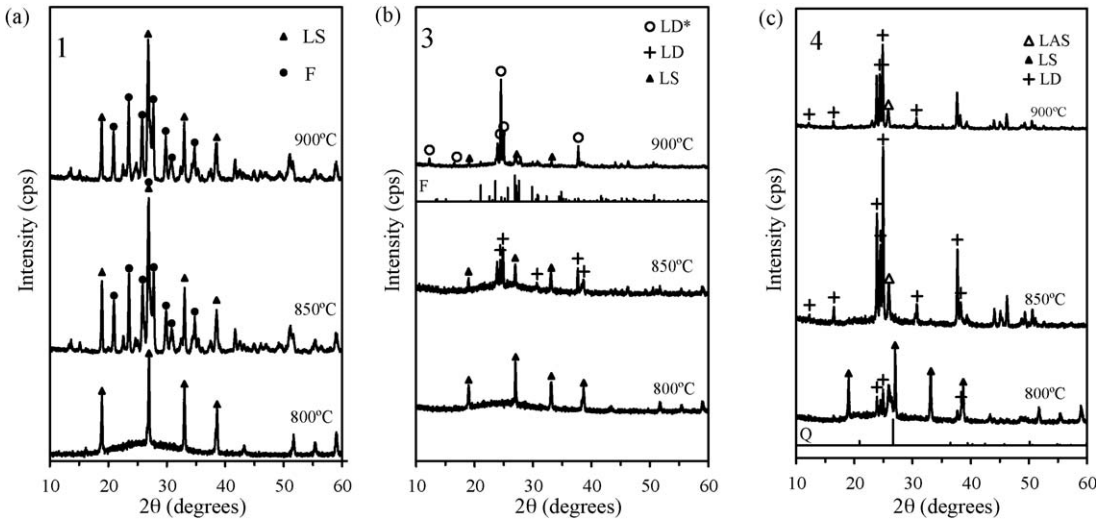

Fig. 2. X-ray diffractograms of glass-powder compacts sintered at different temperatures for 1 h: (a) 1 (full scale of intensity axis: 10,000 cps), (b) 3 (full scale of intensity axis: 7000 cps), and (c) 4 (full scale of intensity axis: 7000 cps). (Full scale of intensity axis: 10,000 cps in (a) and 7000 cps in (b) and (c); for the abbreviation of the phases and the ICDD cards of the plotted patterns, see the legend of Table 3.

metasilicate (LS, Li_2SiO_3) was exclusively registered at 800 °C. The diffractograms of Fig. 3 confirm that LS forms already at 700 °C and is the primary crystalline phase of GC 1 after prolonged heat treatments for 3.5 h and 14 h, which allowed us to assign the crystallization peak of the corresponding DTA plot to LS formation (Fig. 1). Intensive precipitation of potassium feldspar orthoclase (F, $KAlSi_3O_8$), as secondary phase, occurs at 850 °C (Fig. 2a). The evolution of crystalline regimes in the glass-powder compacts 1 and 2 over increasing temperature is summarized in Table 3, where the major phases (i.e. these with strong XRD peaks) are indicated with bold. In GC 2, LS, lithium aluminium silicate (LAS), and LD were crystallized between 800 °C and 900 °C. LD does not form in GC 1 but it was a minor phase in GC 2.

Formation of Li_2SiO_3 as the main crystalline phase in the GCs 1 and 2 stimulated investigation on lithium disilicate synthesis via solid-state reaction between Li_2SiO_3 and SiO_2. In particular, the compositions 1–20, 2–20, 1–30 and 2–30 were prepared from mixtures of colloidal amorphous silica (assuming addition dry weight of SiO_2 from the suspension) and fine glass powders of the glasses 1 and 2 in weight ratio 20/100 and 30/100. The DTA plots of 1–20, 2–20, 1–30, and 2–30 compositions (Fig. 1), exhibit a single crystallization peak, which shifts to higher temperatures, as compared to the parent glasses 1 and 2. The X-ray analysis (Table 3) confirms the formation of LD as the main crystalline phase, and LS and orthoclase (F) as minor phases, in compositions 1–20 and 1–30 at the temperature range of 800–900 °C, supporting the occurrence of the solid-state reaction of Eq. (1). The intensity of the X-ray peaks of quartz, registered with high intensity in the diffractograms at 800 °C and 850 °C (not shown) disappeared at 900 °C (Table 3), indicating the active role of silica in the formation of the desired LD phase predicted by Eq. (1). In the light of these results, samples of the compositions 2–20 and 2–30 were sintered only at 900 °C. X-ray analysis showed the same phase assemblage (to the compositions 1–20

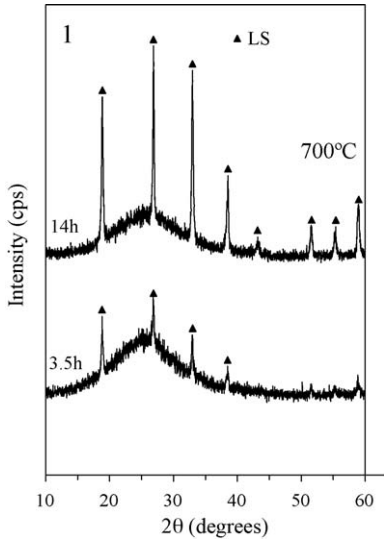

Fig. 3. X-ray diffractograms of glass-powder compacts with composition 1 heat-treated at 700 °C for 3.5 h and 14 h. (ICDD card of Li_2SiO_3 04-008-8713; full scale of intensity axis 3500 cps).

Table 3
Evolution of crystalline phases over increasing temperature for the investigated glass-ceramics.

Composition	800 °C	850 °C	900 °C
1	**LS**	**LS**, F	**LS**, F
1–20	**LS**, **Q**, LD	**LD**, LS, Q, F	**LD**, LS, F
1–30	**LD**, Q, LS, F	**LD**, Q, LS, F	**LD**, LS, F
2	**LS**, LAS	**LS**, LAS, LD	**LS**, LAS, LD
2–20			**LD**, LS, S
2–30			**LD**, LS, S
3	**LS**	**LD**, LS	**LD***, F, LS
4	**LS**, Q, LD	**LD**, Q, LAS	**LD**, LAS

LS: Lithium metasilicate (Li_2SiO_3, ICDD card 04-008-8713); LD: lithium disilicate ($Li_2Si_2O_5$, 00-040-0376; LD*: 00-049-0803); LAS: lithium aluminum silicate ($LiAlSi_3O_8$, 00-035-0794); F: potassium feldspar ($KAlSi_3O_8$, 01-071-0957); S: sanidine ($KALSi_3O_8$, 00-025-0618); Q: quartz (SiO_2, 01-076-0912). The major phases appear in bold.

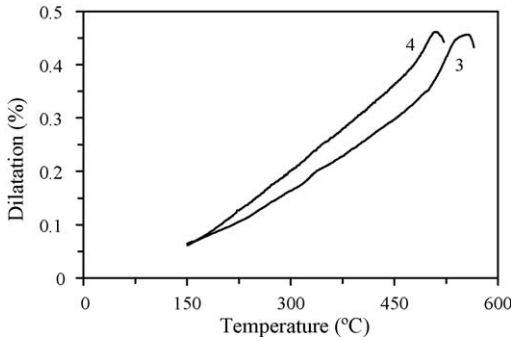

Fig. 4. Dilatometry curves of as-cast and annealed bulk glasses 3 and 4.

and 1–30), but sanidine (which is a high temperature polymorph of K-feldspar [3]) was registered instead of orthoclase.

Transparent and colourless glasses 3 and 4 were prepared by standard melting technique at 1500 °C and 1550 °C for 2 h, respectively. The crystallization effect was weaker but peaked at the same temperatures with the glasses 1–30 and 2–20 (Fig. 1). From the dilatometry curves, plotted in Fig. 4, the glass transition temperatures (T_g), the dilatometric softening points (T_s) and CTE of the glasses 3 and 4 were determined (Table 4). With regard to the evolution of crystalline regime (Table 3), after heat treatment at 800 °C, LS predominantly forms in GC 3 (Fig. 2b), while LS co-exists with Q and LD in GC 4 (Fig. 2c). LD predominates after sintering at 850 °C and 900 °C, evidently occurring via the precursor phase of LS. LS and orthoclase (F) in GC 3, and LAS in GC 4 were the minor crystalline phases. White coloured GCs 3 and 4, featuring self-glazing effect and translucence, were obtained after sintering at 850 °C and 900 °C. Table 5 summarizes the properties of GCs 3 and 4.

The observation of the microstructures of the GCs by SEM revealed different morphologies of the crystals developed. The typical microstructure of GC 1 sintered at 800 °C (Fig. 5a) features dendrite configuration of LS crystals, embedded in glassy phase that agrees fairly well to Stookey studies [1,30] in

Table 4
Characteristic temperatures (in °C) and CTE (for the range 200–400 °C) of the investigated glasses 3 and 4, determined by dilatometry (Fig. 4).

Glass	T_g (°C)	T_s (°C)	CTE ($\times 10^{-6}$ K^{-1})
3	480	550	8.00
4	470	512	10.23

Table 5
Properties of the glass-ceramics 3 and 4 sintered at different temperatures for 1 h.

Property	T (°C)	3	4	n
Density (g/cm^3)	850	2.34 (0.01)	2.35 (0.02)	10
	900	2.33 (0.01)	2.34 (0.01)	10
Shrinkage (%)	850	16.9 (0.2)	16.6 (0.1)	5
	900	16.6 (0.3)	16.7 (0.3)	5
3-Point bending strength (MPa)	850	165.3 (25.6)	151.9 (10.6)	10
	900	162.5 (30.7)	201.4 (14.0)	10
Vickers microhardness (GPa)	900	5.27 (0.48)	5.34 (0.40)	10
CTE ($\times 10^{-6}$ K^{-1}) (200–700 °C)	900	8.46	9.21	1
Chemical durability (μg/cm^2)				
16 h	900	100	80	5
32 h		390	200	5

n: number of samples tested.

SiO_2–Li_2O system. The main characteristic of the microstructure of the GCs of 3 and 4 sintered at 900 °C (Fig. 5b, c) is the regions free of superficial glassy phase at which interlocking fine-grained (of submicron size) LD crystals join one to the other forming endless chains.

4. Discussion

As it has been thoroughly presented in Section 1, in dentistry, much effort has been addressed at developing LD-based GCs in the recent years [1,2,4–10,17–29]. Nucleation and crystallization of LD are optimally favoured with 1.5–2.5 mol% P_2O_5 [22,23,31], resulting in fine-grained interlocking microstructures of high mechanical strength. The present work attempted a novel approach for producing LD-based GCs via sintering and crystallization of glasses in the quaternary SiO_2–Al_2O_3–K_2O–Li_2O system with no addition of nucleating agents. The SiO_2 content in the compositions where LD was the main crystalline phase was significantly higher than in compositions commonly used for producing LD GCs, including the commercial IPS Empress®2 [1,19,22,32].

This work endeavoured production of LD GCs from the hypothetical L–LD system. The formation of LS, as the main crystalline phase in the GCs 1 and 2 for all the investigated temperatures, challenged us to investigate the eligibility of the solid-state reaction of LS and silica for LD formation, according to Eq. (1). The experimental results (XRD, DTA) from the second (1–20, 1–30, 2–20, 2–30) and the third series (3, 4) of compositions confirmed the hypothesis of Eq. (1) occurrence between 800 °C and 900 °C. These findings agree fairly well to earlier studies on nucleation and crystallization of LD in Al_2O_3-

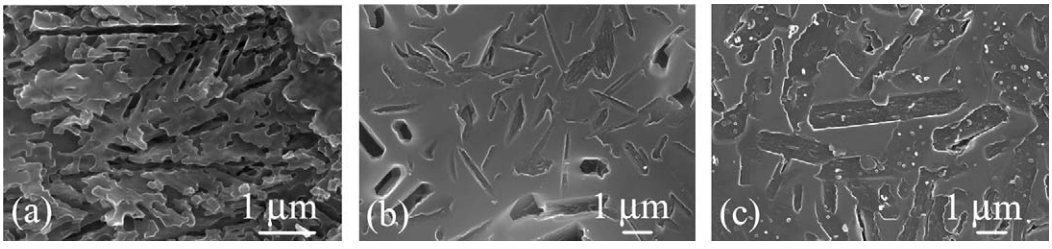

Fig. 5. Typical microstructures of sintered (for 1 h) glass-ceramics: (a) 1 (800 °C); (b) 3 (900 °C); and (c) 4 (900 °C); after chemical etching with HF solution.

containing multi-component systems [1,27,32]. The presence of the phases of orthoclase, sanidine, LS, and LAS has been also reported in other GC compositions [1,3,19–21,33].

The fine-grained interlocking microstructures in the GCs 3 and 4 (Fig. 5b, c) conferred the final products with high mechanical strength (Table 5) in comparison with LS-based parent GCs 1 and 2 (Table 2). Determination of the particular influence of the minor crystalline phases (such as lithium metasilicate potassium feldspar and lithium aluminium silicate) and the residual glass (Fig. 2b and c) on the properties of the LD-based GCs 3 and 4 (Table 5) is beyond the scope of the present paper.

With regards to the prospects of the new GCs for producing dental restorative materials, the compositions 3 and 4 seemingly feature the highest potential due to their overall evaluation of mechanical, chemical, and aesthetic properties. The 3-point bending strength is lower than the commercial IPS Empress®2 (400 ± 40 MPa [1], 306 ± 29 MPa [34]), but comparable to some experimental LD GCs (190–234 MPa [1,19–21], 204.75 ± 49.81 MPa [35], 303 ± 49 MPa [33]). It is believed, however, that hot pressing can significantly improve bending strength of the investigated GCs [1]. Microhardness of GCs 3 and 4 is lower than commercial L-based OPC® (commercial Optimal Pressable Ceramic, Jeneric Pentron, Wallingford, USA, 7.28 ± 0.62 GPa) and IPS Empress® (6.94 ± 0.79 GPa) GCs [36], but comparable to commercially available LD GCs (OPC® 3G™, Pentron® Corporation, 5.77 ± 0.20 GPa [37]). Chemical durability is weaker than IPS Empress®2 (50 $\mu g/cm^2$), but more resistant than IPS Empress® (122 $\mu g/cm^2$) for layering technique [1].

Concerning the potential suitability of the studied GCs for the production of dental materials, the results of the present study qualify compositions 3 and 4 for further consideration and experimentation, such as tests of wear resistance and *in vitro* and *in vivo* toxicity, addition of agents for adjusting colour and translucence etc., which are currently underway and will be reported in a forthcoming publication.

5. Conclusions

The feasibility of the solid-state reaction between lithium metasilicate and silica to lithium disilicate formation in the SiO_2–Al_2O_3–K_2O–Li_2O system was demonstrated.

Production of LD-based glass-ceramics via sintering and crystallization of glass-powders compacts, having a SiO_2 content, which is considerably higher than in conventional LD GCs, was successfully achieved.

The produced LD glass-ceramics developed fine-grained interlocking microstructure, which confers to them high mechanical strength and chemical durability. Hence they have potential for further consideration and experimentation, and for producing materials for dental applications.

Acknowledgments

The participation of S. Agathopoulos has been in the framework of the Project ENTER 04EP26, co-financed by E.U.-European Social Fund (75%) and the Greek Ministry of Development-GSRT (25%). I. Kansal has been gratefully funded by a fellowship of CICECO-Portugal.

References

[1] W. Höland, G. Beall, Glass-Ceramic Technology, Am. Ceram. Soc., Westerville, Ohio, 2002.
[2] R.W. Wassell, A.W.G. Walls, J.G. Steele, Crowns and extra-coronal restorations: materials selection, Br. Dent. J. 191 (2002) 199–211.
[3] M.J. Cattell, T.C. Chadwick, J.C. Knowles, R.L. Clarke, The crystallization of an aluminosilicate glass in the K_2O–Al_2O_3–SiO_2 system, Dent. Mater. 21 (2005) 811–823.
[4] R.L. Ibsen, T.C. Chadwick, S.A. Pritchard, Strong dental porcelain and method for its manufacture, US Patent 5,009,709 (1991).
[5] B. Burk, A.P. Burnett, Leucite containing porcelains and method of making same, US Patent 4,101,330 (1978).
[6] M. Weinstein, S. Katz, A.B. Weinstein, Fused porcelain to metal teeth, US Patent 3,052,982 (1962).
[7] D. Nathanson, Principles of porcelain use as an inlay/onlay material, in: D.A. Garber, R.E. Goldstein (Eds.), Porcelain and Composite Inlays and Onlays, Aesthetic Posterior Restorations, Quintessence Publishing Co., Inc., Carol Stream, IL, 1994, pp. 32–36.
[8] A. Wohlwend, P. Schaerer, The Empress technique for the fabrication of full ceramic crowns, inlays and veneers, Quintessenz Zahntech. 16 (1990) 966–978.
[9] W.H. Mormann, A. Bindl, The cerec 3—a quantum leap for computer-aided restorations: initial results, Quintessence Int. 31 (2000) 699–712.
[10] W. Höland, M. Schweiger, M. Frank, V. Rheinberger, A comparison of the microstructure and properties of the IPS Empress® 2 and the IPS Empress® glass-ceramics, J. Biomed. Mater. Res. (Appl. Biomater.) 53 (2000) 297–303.
[11] P.W. McMillan, 2nd ed., Glass-Ceramics, Academic Press, New York, 1979.
[12] P.E. James, Kinetics of crystal nucleation in silicate glasses, J. Non-Cryst. Solids 73 (1985) 517–540.
[13] T.G. Headley, R.E. Loehman, Crystallization of glass-ceramics by epitaxial growth, J. Am. Ceram. Soc. 67 (1984) 620–625.
[14] E.D. Zanotto, Metastable phases in lithium disilicate glasses, J. Non-Cryst. Solids 219 (1997) 42–48.
[15] R. Ota, N. Mashima, T. Wakasugi, J. Fukunaga, Nucleation of Li_2O–SiO_2 glasses and its interpretation based on a new liquid model, J. Non-Cryst. Solids 219 (1997) 70–74.
[16] C.S. Ray, D.E. Day, W. Huang, K. Lakshmi Narayan, T.S. Cull, K.F. Kelton, Non-isothermal calorimetric studies of the crystallization of lithium disilicate glass, J. Non-Cryst. Solids 204 (1996) 1–12.
[17] J.M. Barrett, D.E. Clark, L.L. Hench, Glass-ceramic dental restoration, U.S. Patent 4,189,325 (1980).
[18] J.M. Wu, W.R. Cannon, C. Panzera, Castable glass-ceramic composition useful as dental restorative, US Patent 4,515,634 (1985).
[19] L.M. Echeverria, New lithium disilicate glass-ceramics, Bol. Soc. Esp. Ceram. Vid. 5 (1992) 183–188.
[20] G.H. Beall, Glass-ceramics: recent development and application, Ceram. Trans. 30 (1993) 241–266.
[21] G.N. Beall, Design of glass-ceramics, Solid State Sci. 3 (1989) 333–354.
[22] C.S. von Clausbruch, M. Schweiger, W. Höland, V. Rheinberger, The effect of P_2O_5 on the crystallization and microstructure of glass-ceramics in the SiO_2–Li_2O–K_2O–ZnO–P_2O_5 system, J. Non-Cryst. Solids 263–264 (2000) 388–394.
[23] M. Schweiger, Microstructure and mechanical properties of a lithium disilicate glass-ceramic in the SiO_2–Li_2O–K_2O–ZnO–P_2O_5 system, Glastech. Ber. Glass Sci. Technol. 73 (2000) 43–50.
[24] W. Höland, Materials science fundamentals of IPS Empress®2 glass-ceramics, Ivoclar-Vivadent Report 12 (1998) 3–10.
[25] M. Frank, M. Schweiger, V. Rheinberger, W. Höland, High-strength translucent sintered glass-ceramics for dental application, Glasstech. Ber. Glass Sci. Technol. 71C (1998) 345–348.

[26] M. Schweiger, M. Frank, C.S. von Clausbruch, W. Höland, V. Rheinberger, Microstructure and properties of pressed glass-ceramic core to zirconia post, Quint. Dent. Technol. 21 (1998) 73–79.
[27] J.R. Jacquin, M. Tomozawa, Crystallization of lithium metasilicate from lithium disilicate glass, J. Non-Cryst. Solids 190 (1995) 233–237.
[28] C.S. von Clausbruch, M. Schweiger, W. Höland, V. Rheinberger, The effect of P_2O_5 on the crystallization and microstructure of glass-ceramics in the SiO_2–Li_2O–K_2O–ZnO–P_2O_5 system, Glastech. Ber. Glass Sci. Technol. 74 (2001) 223–229.
[29] W. Höland, V. Rheinberger, E. Apel, C. van Hoen, Principles and phenomena of bioengineering with glass-ceramics for dental restoration, J. Eur. Ceram. Soc. 27 (2007) 1521–1526.
[30] S.D. Stookey, Chemical machining of photosensitive glass, Ind. Eng. Chem. 45 (1953) 115–118.
[31] M.H. Lewis, J. Metcalf-Johansen, P.S. Bell, Crystallization mechanism in glass-ceramics, J. Am. Ceram. Soc. 62 (1979) 278–289.
[32] E. Apel, C. van Hoen, V. Rheinberger, W. Höland, Influence of ZrO_2 on the crystallization and properties of lithium disilicate glass-ceramics derived from a multi-component system, J. Eur. Ceram. Soc. 27 (2007) 1571–1577.
[33] D.U. Tulyaganov, S. Agathopoulos, H.R. Fernandes, J.M.F. Ferreira, Synthesis of lithium aluminosilicate glass and glass-ceramics from spodumene material, Ceram. Int. 30 (2004) 1023–1030.
[34] M. Guazzato, M. Albakry, S.P. Ringer, M.V. Swain, Strength, fracture toughness and microstructure of a selection of all-ceramic materials. Part I. Pressable and alumina glass-infiltrated ceramics, Dent. Mater. 20 (2004) 441–448.
[35] J.L. Drummond, T.J. King, M.S. Bapna, R.D. Koperski, Mechanical property evaluation of pressable restorative ceramics, Dent. Mater. 16 (2000) 226–233.
[36] C.M. Gorman, W.E. McDevitt, R.G. Hill, Comparison of two heat-pressed all-ceramic dental materials, Dent. Mater. 16 (2000) 226–233.
[37] I.L. Denry, J.A. Holloway, Elastic constants, Vickers hardness, and fracture toughness of fluorrichterite-based glass-ceramics, Dent. Mater. 20 (2004) 213–219.